FLOW STRUCTURE WITH FILM BOILING IN VERTICAL TUBES

É. K. Kalinin and V. P. Firsov

UDC 536.423.1:536.483

The authors present results of a study of the structure, hydrodynamics, and heat transfer with film boiling of liquid nitrogen in vertical channels.

The heat transfer and the hydrodynamics in film boiling in channels are substantially interconnected and determined by the flow regime. Therefore, in the study of thermal and hydrodynamic processes in film boiling, and in the construction of efficient and reliable methods of computing these one must investigate conditions under which each film boiling regime is generated and changed, its structure and the mechanism of the physical processes.

This matter has been the subject of a large number of investigations, e.g., [1-10], but many aspects of the problem have not been studied. There are no reliable numerical data on the flow structure and the interphase interaction, on the conditions for regime change, and so on.

The present experimental investigation was undertaken to study precisely these questions.

The experiments were conducted in liquid nitrogen in tubes of length from 0.2 to 3.03 m, of diameter 12, 19, 35, and 70 mm, with upward flow of heat transfer agent, and of diameter 12 and 19 mm with downward flow under study and unsteady cooling conditions. Under steady conditions the channel was heated electrically by a current of mains frequency, and under unsteady conditions a previously heated section was cooled until the film boiling crisis set in. The range of variation of the regime parameters was: mass flow velocity 40-3500 kg/m^2·sec; pressure 0.12-0.55 MN/m^2; underheat of the liquid at the inlet 0.5-20 K; heat flux density 15-190 kW/m^2; maximum channel wall temperature 800 K.

Along the channel we measured [9]: the temperature of the flow and the walls, the pressure and the pressure drop, the volume flow rate of liquid, the heater current and the voltage drop, and the mass vapor content (by the helium indicator method [10]). The presence of droplets of diameter more than 5 μm was determined from the readings of a photoelectric sensor [9]. At the channel outlet there were quartz electrically heated sections of length up to 100 mm, in which we took high-speed pictures of the flow and photographs using a two-pulse light source [9]. With this method and automation of the experiment we could determine the following parameters along the channel to the accuracy shown: temperature and heat flux under steady conditions ± 0.25 and $\pm 2\%$, respectively, and ± 0.3 and $\pm 5.5\%$ under steady conditions; liquid mass flow rate $\pm 1.5\%$; pressure and pressure drop ± 2 and $\pm 0.5\%$; equilibrium mass vapor content $\pm 5\%$ for the steady experiments and $\pm 8\%$ for the unsteady; mass vapor content $\pm 6\%$; velocity of the vapor and the liquid ± 7 and $\pm 12\%$; size of droplets ± 20 μm. The errors shown are for a confidence level of 0.95.

By comparing the experimental results with the photographs and the high-speed pictures we could identify the following characteristics of the flow regime for film boiling and determine their structure: self-similar and nonsimilar rod flow [5], transition flow, disperse-annular, an disperse. Figure 1 shows the characteristic flow structures in these regimes, with an indication of the directions of the mass force vectors and the flow velocity vectors.

We shall consider them in sequence. In the rod flow regime of film boiling the generally underheated jet of liquid is separated from the wall by a film of vapor. The heat flux going to heating the vapor q_v, to evaporation q_i, and to heating the liquid q_ℓ are self-regulated in such a way that in each section of the vapor film the temperature drops through the film from T_w at the wall to T_s at the phase interface. The value of q_ℓ is determined

Sergo Ordzhonikidze Moscow Aviation Institute. Translated from Inzhenerno-Fizicheskii Zhurnal, Vol. 53, No. 6, pp. 885-892, December, 1987. Original article submitted April 3, 1987.

0022-0841/87/5306-1363$12.50

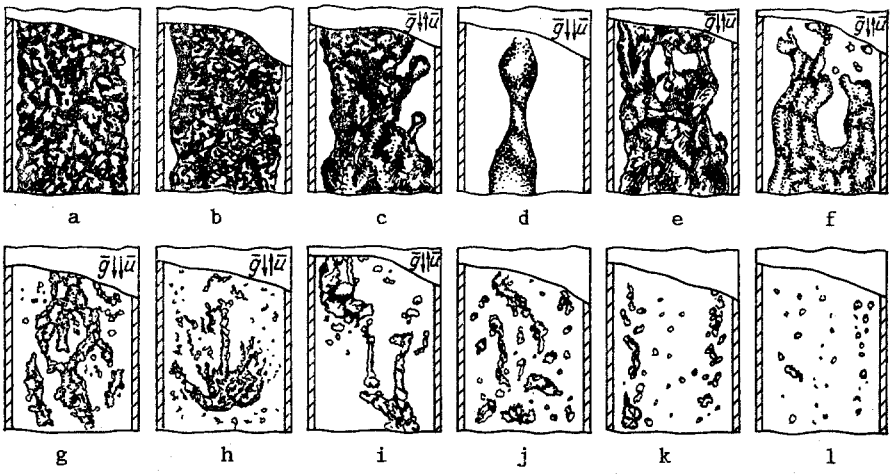

Fig. 1. Flow structure in film boiling in vertical tubes: a-c) rod flow regime; d) rod regime with downward flow with ρu = 100 kg/m²·sec; e) rod regime with slight underheat of the liquid ($T_s - T_\ell$ = 1.5 K); f) decay zone for upward flow with ρu = 70 kg/m²·sec; g) transition regime with upward flow; h-j) transition regime for upward flow; k) disperse-annular regime; l) disperse regime.

by the underheat of the liquid, its level of turbulence and the physical properties. For a specific combination of liquid underheat ($T_s - T_\ell$), temperature head ($T_w - T_s$), and jet turbulence level q_ℓ can be so large that for it to transmit through the vapor film the film must be thin. Then $q_w \approx q_\ell \gg +q_v$. This is the self-similar rod flow regime (Fig. 1a), in which q_w is practically independent of ($T_w - T_s$).

With a decreased underheat underheat (Fig. 1b-e) q_ℓ falls, and the film thickness, and consequently q_i and q_v increase. The nonsimilar rod flow regime sets in. In our tests it was confirmed that if we take $1 < q_w/q_\ell \leq 1.1$ as the boundary between these regimes, this corresponds to obtaining a value of temperature head of $\Theta_1 = c_{pv}(T_w - T_s)/r_i$:

$$\Theta_1 = 0{,}0115\,\frac{\psi^{0,5}}{1+0{,}3L+1{,}3\exp(-0{,}4L)}\left(\mathrm{Re}_\ell\,\frac{\rho_\ell\mu_\ell}{\rho_{vs}\mu_{vs}}\right)^{0,25}, \tag{1}$$

where

$$L=\psi\,\frac{\rho_\ell}{\rho_{vs}}\left(\frac{2\rho_{vs}\sigma R_0}{\mu_{vs}^2}\right)^{0,7}\cdot 10^{-5},\quad \psi=\frac{c_{pl}(T_s-T_\ell)}{r_i}.$$

In the nonsimilar region, where the vapor film is usually turbulent and rather thick, oscillations arise at the surface of the jet with increase of the jet Reynolds number and the degree of shear between the phases. These lead to the formation of wave outbursts, jets with overconstruction, and drops (Fig. 1e). Vapor voids arise, entrained into the flow core (see Fig. 1e), where they are partially or fully condensed. For $\varphi > 0.3$ these vapor formations cannot condense and an annular structure of liquid rod flow forms, especially for large ρu and q_w.

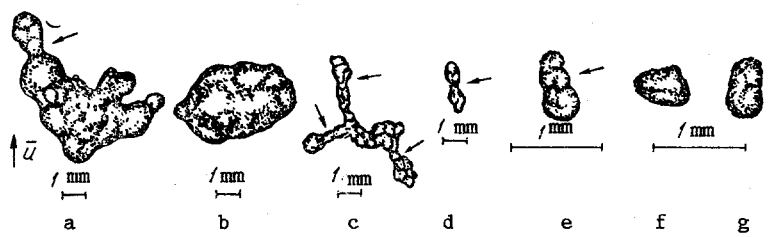

Fig. 2. Shape and size of liquid formations and drops: a-c) transition regime; d-g) disperse-annular and disperse.

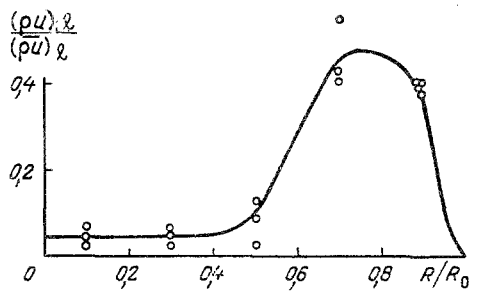

Fig. 3. Variation of the ratio of local mass flow rate to the total rate over the section of a channel of diameter 19 mm in the disperse-annular regime: $\overline{\rho u}$ = 120-200 kg/m²·sec; P = 0.25 MPa.

In downward flow with $\overline{\rho u} < 70$ kg/m²·sec, shear the shear is negative, long-wave surface waves predominate (Fig. 1d). The boundary for existence of the rod-flow regime is usually φ = 0.6-0.7. In this region of liquids the rod breaks down, as is shown in Figs. 1f-g. In downward flow and for small mass flow rates the rod breaks down into coarse drops, which can be seen in Fig. 1d. The transition regime of film boiling sets in.

Breakdown of the rod flow regime can also occur for $\varphi < 0.6$ with strong oscillations of flow rate and pressure accompanying the process of filling and emptying the lines, and dependent on specific details.

Typical flow structures in transition flow are shown in Fig. 1g for downward flow and in Fig. 1g-j for upward flow. The shapes of the liquid formations are shown in Fig. 2a-c, and in downward flow these formations are larger (Fig. 2a) and their breakdown proceeds more slowly.

On breakdown of the liquid rod there is a sharp increase of the liquid surface and on it there is q_w going to evaporate the liquid and the heat expended in the heated vapor. Here the heat flow going to evaporation can exceed q_w. This is accompanied by intense vapor generation, especially in the wall zone, and by acceleration of the vapor and the entire flow. The vapor, being the light phase, tends towards the flow core, and the large liquid formations are either rapidly broken up, or are pushed to the wall where the vapor velocity and the shear are less.

For

$$\Gamma \geqslant 0{,}5 \cdot 10^{-5} \text{ and } \mathrm{Lp}_* \geqslant 6{,}5 \cdot 10^{-2}\, \Gamma^{0{,}4} \tag{2}$$

from the transition regime or directly from the angular structure of the rod regime is formed the disperse-annular for which there is typically an increased concentration of drops near the wall (Fig. 1k).

Up to 80% of the liquid flow is concentrated in this regime in the wall zone (Fig. 3), with a maximum for R/R_0 = 0.6-0.8.

The disperse-annular flow structure exists for mass flow rates above 100 kg/m²·sec. Up to 80% of the liquid is evaporated along the channel in this regime. Turbulent migration of drops [11] also promotes the formation of this flow regime. The disperse-annular structure is not a consequence of flow swirl. When we eliminated flow swirl in our tests (we set up rectifying gratings at the channel inlet) the formation of this structure continued unchanged.

For

$$\mathrm{Lp}_* \geqslant 2{,}3 \cdot 10^{-3} \text{ and } \Gamma \geqslant 0{,}5 \cdot 10^{-5} \tag{3}$$

the disperse-annular regime undergoes transition to the disperse regime (see Fig. 1ℓ) because of evaporation and breakdown of drops near the wall.

For

$$\mathrm{Lp}_* \geqslant 0{,}3 \cdot 10^{-3} \text{ and } \Gamma < 0{,}5 \cdot 10^{-5} \tag{4}$$

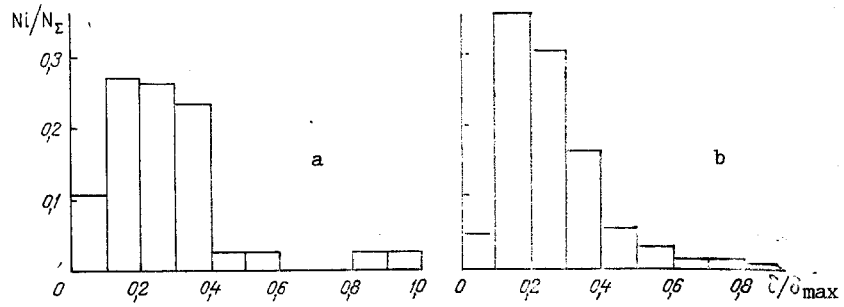

Fig. 4. Histograms of distribution of drops by size in the disperse-annular regime (a) and the disperse regime (b).

the disperse regime arises immediately from the transition regime, and for small flow rates ($\rho u < 70$ kg/m^2·sec) and upward motion it arises directly from the rod flow regime (Fig. 1f). In the latter case at the end of the rod one or several jets are formed which break up into drops, pushed upstream by the vapor. The region of rod flow breakdown fluctuates along the channel, and the jets cause a swirling random motion.

Drops are formed in all regimes of film boiling, including rod flow (Fig. 1d-f). There is a predominance of "thread-shaped" structures orientated along the flow (Fig. 2c-e). For downward flow with small ρu large liquid formations are typical (Fig. 2a).

The nature of the drop distribution by size is shown in histogram form for the disperse-annular regime in Fig. 4a, and for the disperse regime in Fig. 4b. In Fig. 4a we can note the typical bimodal distribution, which is determined by the annular flow structure.

Analysis of the experiments has shown that the distribution by drops by size can be described by the Nukiyama-Tanasava [12] distribution

$$f(\delta) = \tilde{A}\,\tilde{\delta}^{a} \exp\left(-(a/b)\,\tilde{\delta}^{b}\right) \delta_{*}^{-1} \tag{5}$$

with a = 1 and b = 0.5 (3 + th (3(10^3 Lp$_*$ − 1))).

Equation (5) was obtained with a scatter of ±20%, and b varied from 1 to 2. The value b = 1 is typical for the beginning of formation of the disperse-annular regime and agrees with the data of the experiments of [6], and b = 2 is typical for the developed disperse regime and agrees with the data of [12] for evaporating disperse flows.

The use of the Weber number $We = \rho_v(u_v - u_\ell)^2\delta_*/\sigma$ (where δ_* is the characteristic drop size) as a criterion of drop division does not always give satisfactory results and is more suitable for crude estimates. A correlation of the test data has shown that We based on the mean drop diameter varied from 1 in the disperse-annular regime to 6 in the disperse regime. But if we take the size to be the Zauter diameter, then We varies from 1.25 to 7.5, respectively. When We is defined according to maximum drop diameter its value is close to 12.

To generalize and to calculate the size of drops we used a mechanism of drop breakdown under the action of large-scale turbulent fluctuations of vapor [13]. An empirical dependence for calculating the mean-volume drop diameter, correlating the test data with a scatter of ±35% has the form

$$\frac{\delta_{30}}{\delta_{mT}} = 0{,}5\,\mathrm{th}\,(500\,\mathrm{Lp}_*\,(1 - 0{,}14\,\mathrm{sch}\,(3\cdot 10^3\,\mathrm{Lp}_*))), \tag{6}$$

where

$$\delta_{mT} = \frac{\sigma}{1{,}69\rho_v v_*^2} + \frac{\mu_\ell}{1{,}3\rho_v v_*}\sqrt{\frac{\rho_v}{\rho_\ell}}. \tag{7}$$

The size of the maximum drops in the flow is correlated, with a scatter of ±50%, by the following dependence:

$$\frac{\delta_{max}}{\delta_{mT}} = 0{,}1\,\mathrm{Lp}_*^{-0.4}. \tag{8}$$

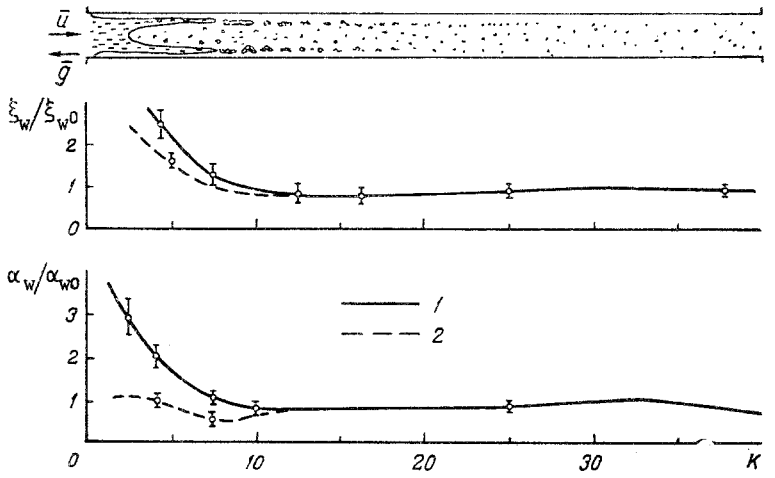

Fig. 5. Dependence of the ratios of measured values of the coefficients of heat transfer and friction at the wall of a channel of diameter 12 mm, as calculated from relations for single-phase flow, on the parameter K, for ρu = 200 kg/m^2·sec and P = 0.25 MPa: 1) upward flow; 2) downward flow.

The ratio δ_{max}/δ_{mT} according to Eq. (8) varies from 2 for the disperse-annular regime to 1 for the disperse regime.

The tests have shown that the velocity of drops in the flow does not depend on their size, with an accuracy of ±12%, which agrees with the conclusions of [6]. A small drop (up to 10%) in their velocity in the wall zone is observed for the disperse-annular regime [9]. This allows the one-speed model of drop motion to be used for the calculations.

A correlation of results of experiments on friction at the interphase surface has shown that the drag of drops in the disperse-anngular regime can appreciably exceed (by a factor of 10-12) values characteristic for solid spheres. These differences are due to deformation of the drops, the flow turbulence, and the nonuniformity of drop distribution over the channel. The test data are correlated with an error of ±60% by the dependence:

$$c_D = \begin{cases} 9\,(10^3\,\mathrm{Lp}_*)^{-2}\,c_{D0} & \text{for } \mathrm{Lp}_* \leqslant 3\cdot 10^{-3}, \\ c_{D0} & \text{for } \mathrm{Lp}_* > 3\cdot 10^{-3}, \end{cases} \tag{9}$$

where

$$c_{D0} = \frac{24}{\mathrm{Re}_\delta} + \frac{4{,}4}{\sqrt{\mathrm{Re}_\delta}} + 0{,}32. \tag{10}$$

The convective heat transfer to the drops in the disperse regime is correlated, with an error of ±50%, by the relation used in [3], for a specific vapor temprature T_f and introducing a correction for evaporation [14]:

$$\mathrm{Nu}_{f\delta} = (2 + 0{,}55\mathrm{Re}_{f\delta}^{0,5}\,\mathrm{Pr}_f^{0,33})\,(1 + 0{,}92\Theta)^{-0,7} \tag{11}$$

where $\Theta = (i_v - i_s)/r_i$. In the transition region and the disperse-annular regime the evaporation rate increases up to a factor of 10 compared with the value calculated according to Eq. (11). This is associated with direct evaporation of liquid formations close to the heat-emitting surface [15].

Heat Transfer and Hydraulic Drag. A comparison of local values of heat transfer and friction at the channel wall with values calculated from relations for gas flow in a tube using data on flow structure is shown in Fig. 5. For upward flow in the rod flow and annular regimes (K < 10) the heat transfer and friction considerably exceed the values calculated for a gas using local values of mean-mass temperature and vapor velocity. For the disperse-annular regime (K ≥ 10) an insignificant drop of friction and heat transfer (up to 25%) compared with single-phase flow is observed. This effect is evidently due to decrease of the

intensity of turbulence of the vapor because of an increased concentration of drops in the wall zone. The appearance of fine-scale fluctuations in gas curtain flow in tubes was noted in [16]. For reduced drop concentration the ratio of the measured and the calculated values is observed to tend to 1.

For downward flow in the region of the transition regime, due to an increase of the volume vapor content compared with upward flow, the calculated and measured values of heat transfer and friction are close.

The influence of the temperature factor (T_w/T_v) is noted in the disperse regime ($K > 30$ in Fig. 5) and in downward flow ($K < 10$ in Fig. 5) in the transition regime, because of the large volume vapor content ($\varphi > 0.9$) and the insignificant vapor velocity. The absence of influence of the temperature factor in the disperse-annular regime can be explained by the presence of heat sinks and mass sources in the wall zone, and also by the large turbulence-creating action of drops on the flow.

The results of tests on friction and heat transfer at the channel wall in the disperse-annular and disperse regimes are correlated by the relations

$$\mathrm{Nu}_w = a\,\mathrm{Nu}_0 (T_w/T_v)^b, \tag{12}$$

$$\xi_c = c\xi_0, \tag{13}$$

where

$$\mathrm{Nu}_0 = 0{,}023\,\mathrm{Re}_v^{0,8}\,\mathrm{Pr}_v^{0,43}, \tag{14}$$

$$\xi_0 = 0{,}316\mathrm{Re}_v^{-0,25}. \tag{15}$$

For the disperse-annular regime a = 0.75; b = 0; c = 0.75. In the disperse regime and the transition regime in downward flow a = 1; b = −0.37; c = 1.

NOTATION

P, pressure; ρ, density; u, velocity; i, enthalpy; T, temperature; R, radius; R_0, channel radius; $F = \pi R_0^2$, area of channel cross section; σ, surface tension coefficient; c_p, specific heat at constant pressure; μ, dynamic viscosity; λ, thermal conductivity; r_i, specific heat of vaporization; G, mass flow rate; φ, volume vapor content; x, mass vapor content; q, heat flux density, consant; δ, drop diameter; $\bar{\delta} = \delta/\delta_*$, relative drop diameter; δ_*, most probable drop diameter; $v_* = u_v\sqrt{\xi_0/8}$, dynamic velocity; $\mathrm{Lp}_* = \mu_\ell v_*/\sigma\sqrt{\rho_v/\rho_\ell}$, modified Laplace number; We, Weber number; c_D, drop drag coefficient; $\mathrm{Nu} = 2\alpha R_0/\lambda$, Nusselt number; $\mathrm{Nu}_{f\delta} = \alpha_\delta\delta/\lambda_{vf}$, Nusselt number for a drop; $\mathrm{Re} = 2\rho u R_0/\mu$, Reynolds number; $\mathrm{Re}_{f\delta} = \rho_{vf}(u_v - u_\ell)\delta/\mu_{vf}$, Reynolds number for a drop; $\mathrm{Pr} = \mu c_p/\lambda$, Prandtl number; $K = u_v\sqrt{\rho_v}/\sqrt{g\sigma(\rho_\ell - \rho_v)}$, parameter for hydrodynamic stability of gas–liquid systems; $g = 9.81$ m/sec^2, acceleration of free fall; ξ, hydraulic drag coefficient; α, heat-transfer coefficient; $\Gamma = 1/P\ G/F\ q_c/\rho_{vs}r_i$, flow regime change parameter; $f(\delta)$, density of drop distribution by size; $\tilde{A} = \left(\varphi^d\int_0^\infty t^d e^{-t}dt\right)$, normalizing factor; $d = (2 - q)/q$, constant; N, number of drops; $\overline{\rho u} = G/F$, mass flow velocity; $N_i = N_\Sigma\int_{\delta_i}^{\delta_{i+1}} f(\delta)\,d\delta$, number of drops in the i-th group; a, b, c, p, constants. Subscripts: ℓ, liquid; v, vapor; w, wall, s, on the saturation line; *, parameter calculated from the dynamic velocity; 30, mean-volume; max, maximum measured; mT, maximum calculated; o, single-phase; f, parameter defined at temperature $T_f = 0.5\,(T_v + T_s)$; $\sim$, relative value of the quantity; i, group number; −, mean value of a quantity, or vector.

LITERATURE CITED

1. V. F. Laverti and V. N. Rozenau, Teploperedacha, No. 1, 110-120 (1967).
2. J. W. H. Chi and A. M. Vetere, Adv. Cryogen. Eng., 9, 243-253 (1964).
3. R. P. Forslund and V. N. Rozenau, Teploperedacha, No. 4, 32-41 (1968).
4. G. M. Leonova, V. G. Pron'ko, and Ya. G. Vinokur, Teploenergetika, No. 10, 81-82 (1968).
5. V. K. Koshkin, E. K. Kalinin, G. A. Dreitser, and S. A. Yarkho, Unsteady Heat Transfer [in Russian], Moscow (1973).

6. Kumo, Farello, Ferrari, and Palatsii, Teploperedacha, No. 4, 66-79 (1974).
7. A. A. Kurilenko, S. K. Dymenko, and Yu. S. Kochelaev, Inzh.-Fiz. Zh., 39, No. 3, 442-448 (1980).
8. S. A. Yarkho, N. V. Filin, A. P. In'kov, et al., Heat and Mass Transfer V, Pt. 2 [in Russian], Minsk (1976), pp. 80-89.
9. V. P. Firsov, Heat and Mass Transfer VI, Pt. 1 [in Russian] Minsk (1980), pp. 148-156.
10. G. A. Dreitser, V. P. Firsov, G. N. Sdobnov, and M. G. Kraev, "Thermophysics and hydrogasdynamics of the processes of boiling and condensation," Rep. All-Union Conf., Riga (1985), Vol. II, Part 2, pp. 78-86.
11. E. P. Mednikov, Turbulent Transfer and Deposition of Aerosols [in Russian], Moscow (1981).
12. G. Wallace, One-Dimensional Two-Phase Flow [Russian translation], Moscow (1972).
13. G. A. Hugmark, AIChE, 17, No. 4, 1000 (1971).
14. B. I. Brounshtein and G. A. Fishbein, Hydrodynamics and Mass and Heat Transfer in Disperse Systems [in Russian], Leningrad (1977).
15. A. S. Lyshevskii, Izv. Vyssh. Uchebn. Zaved., Energ., No. 7, 75-81 (1963).
16. A. A. Shraiber, V. N. Milyutin, and V. P. Yatsenko, Hydromechanics of Two-Component Flows with Solid Semidisperse Material [in Russian], Kiev (1980).

OPTICAL INVESTIGATION OF HEAT AND MASS TRANSFER IN VAPOR CONDENSATION FROM VAPOR–GAS MIXTURES

A. G. Usmanov, V. P. Bol'shov,
A. P. Mishchenko, G. Sh. Fatkullin, and
É. S. Sergeenko

UDC 536.423.4

Experimental data on the temperature and concentration fields are obtained by an interferometric procedure in vapor condensation from a vapor–gas mixture and from a vapor–vapor mixture of six working media under natural convection conditions.

The condensation of vapor–gas mixtures and vapor–vapor mixtures forming a homogeneous liquid phase is encountered frequently in practice. However, it has not been adequately studied under the conditions of natural convection. The complex mechanism of the process and experimental difficulties stand in the way.

The presence of a gas in a vapor or the intrusion of another component is known to create diffusion resistance, so that the resistances of the liquid and vapor phases must be taken into account separately. This formulation of the problem requires the determination of the temperature and concentration at the phase interface, along with the temperature and concentration distributions in the vapor phase [1]. We have therefore undertaken experimental measurements of the temperature and concentration fields in a vapor layer.

The optical method is the most practical approach to the solution of the problem. It has the important inherent advantages of quick response and freedom from any disturbance of the investigated process; it also affords the possibility of observing visually the configuration of the vapor boundary layer and the dynamics of its variation under the action of a variety of factors.

To investigate the concurrent processes of heat and mass transfer in vapor condensation from a vapor–gas mixture and from a vapor–vapor mixture on a horizontal cylinder under natural convection conditions, we designed and assembled experimental apparatus using a two-wave polarization schlieren interferometer.

S. M. Kirov Chemical-Technological Institute, Kazan. Translated from Inzhenerno-Fizicheskii Zhurnal, Vol. 53, No. 6, pp. 892-897, December, 1987. Original article submitted July 8, 1986.

0022-0841/87/5306-1369$12.50